

Oncolytic Herpes Simplex Virus Mutants Exhibit Enhanced Replication in Glioma Cells Evading Temozolomide Chemotherapy through Deoxyribonucleic Acid Repair

Manish Aghi, M.D., Ph.D., Samuel Rabkin, Ph.D., and Robert L. Martuza, M.D.

INTRODUCTION

Engineered oncolytic viruses take advantage of cancer cell mutations and induce selective destruction.^{1–3} We hypothesized that chemotherapy-induced tumor-protective deoxyribonucleic acid (DNA) repair proteins promote oncolytic herpes simplex virus (HSV) replication. Specifically, in this manuscript, we demonstrate that human glioma cells respond to glioma chemotherapeutic temozolomide by expressing DNA repair genes that can be targeted to improve oncolytic HSV therapy.

Glioblastomas are aggressive neoplasms resistant to current treatments, with surgery, radiation, and chemotherapy minimally altering the median survival of the disease (12–15 months) during the past decade.⁴ G207, an oncolytic HSV,³ has deletions of both copies of neurovirulence gene γ 34.5 and an inactivating mutation of U_L39, encoding ICP6, the HSV ribonucleotide reductase (RR) large subunit. These mutations ensure that G207 selectively replicates in and lyses dividing cells, possibly because dividing cells express mammalian RR and growth-arrest DNA damage 34 (GADD34), genes whose products are not yet fully characterized but may regulate the cell cycle^{5,6} and complement G207 mutations. Mammalian RR generates deoxyribonucleotides in place of HSV RR and the GADD34 carboxyl terminus substitutes for the homologous γ 34.5 region.⁷ Intratumoral G207 inoculation has efficacy in glioma animal models and a phase I clinical trial demonstrated safety of intracranial G207 inoculation in glioma patients, with partial radiological responses.^{3,8,9}

Temozolomide, an oral alkylating agent with slight phase II clinical trial efficacy against glioblastoma,¹⁰ spontaneously converts, at nonacidic pH, into its active metabolite, 5-(3-methyltriazene-1-yl)imidazole-4-carboxamide (MTIC), a DNA-alkylating agent that methylates guanines at O6 and N7 positions.¹¹ O6-methylguanine is not itself lethal to cells, but pairs with thymine, triggering mismatch DNA repair, a three-step process involving: 1) mismatched base removal by

N-methylpurine-DNA glycosylase (MPG)¹²; 2) strand cleavage by apurinic/apyrimidic endonuclease; and 3) strand breaks recruit poly(adenosine diphosphate [ADP]-ribose) polymerase (PADPRP), a nick sensor targeting the DNA repair synthetic machinery to damaged DNA.¹² However, if repair fails to keep pace with DNA damage, repetitive futile rounds of mismatch repair create DNA strand breaks, activating the serine/threonine kinase, ataxia-telangiectasia mutated (ATM) and Rad3-related (ATR) during S-phase.¹³ If ATR activation fails to cause cell cycle arrest, subsequent S-phases convert single-strand breaks into double-strand breaks, which activate serine/threonine kinase ATM. Activated ATM promotes cell cycle arrest and apoptosis.¹¹

Unfortunately, many gliomas lack temozolomide sensitivity, primarily because of expression of DNA repair enzyme O6-methylguanine-DNA methyltransferase (MGMT). MGMT, expressed by 20% of gliomas, facilitates temozolomide resistance by removing the alkyl adduct from the O6 position of guanine before mismatch repair begins.^{14,15} MGMT-mediated temozolomide resistance can be partially overcome with O6-benzylguanine (O6BG), an MGMT inactivator proven safe and capable of enhancing temozolomide responsiveness of MGMT-expressing gliomas in phase I clinical trials.¹⁶

Because these new therapies generate only partial responses, glioblastoma treatment requires multimodal therapy. We hypothesized that limitations in temozolomide and G207 glioma treatment could be jointly addressed by using temozolomide-induced DNA repair genes to enhance HSV replication. Although some studies found synergy between oncolytic HSV and chemotherapy,^{17–21} the interaction was usually not quantified or mechanistically explained. Herein, we used Chou-Talalay multiple drug-effect analysis²² to quantify the interaction between temozolomide and oncolytic HSV. We demonstrate: 1) profound synergy between temozolomide and certain oncolytic HSVs in culture; 2) that glioma p53 expression influences MGMT expression; 3) that MGMT expression determines the HSV mutation required for synergy to

occur; 4) a mechanism of interaction: enhanced HSV replication in cells surviving temozolomide treatment by expressing DNA repair genes, which varied with tumoral MGMT expression; and 5) efficacy of combined treatment in vivo with temozolomide and G207.

MATERIALS AND METHODS

Plasmids

The MGMT complementary DNA (cDNA) was obtained from American Type Culture Collection (ATCC, Manassas, VA), and subcloned into the pCDNA3 vector (Invitrogen, Carlsbad, CA). The plasmid pc53-SCX3 contains a cDNA encoding a dominant p53 mutation.²³ The 700-base pair human GADD34 promoter was cloned using a 30 cycle PCR (20 seconds at 98°C, 2 minutes at 68°C per cycle) with the Takara LA Taq Polymerase (Panvera Corporation, Madison, WI), with template DNA isolated from U87 cells (Trizol, according to Invitrogen protocol); forward primer 5'-CAATTGGGGAGGCCAAGGCGGGAGGAT-3'; and reverse primer 5'-GAATTCTAAGAGCAACGAACACAATGGC-3' (Invitrogen). The PCR product was sequenced and inserted in place of the cytomegalovirus (CMV) promoter into the plasmid pCMV-EGFP (kindly provided by T. Kuroda, Charlestown, MA), generating the plasmid pGADD34-EGFP containing the enhanced green fluorescent protein (EGFP) driven by the human GADD34 promoter.

Cell Lines

U87, U373, and T98 human glioblastoma and Vero (African green monkey kidney) cells were obtained from ATCC. The three plasmids, pCDNA3-MGMT, pc53-SCX3, and pGADD34-EGFP, were transfected into U87 cells using lipofectamine according to the manufacturer's protocol (Invitrogen). Clones were isolated in 1 mg/ml G418 (GIBCO; Carlsbad, CA). Clones from the pc53-SCX3 transfection were screened for mutant p53 expression using an enzyme-linked immunosorbent assay (ELISA) kit (Calbiochem, San Diego, CA), with the clone expressing the largest amount of mutant p53 designated U87/mp53. Clones from the pGADD34-EGFP transfection were screened by flow cytometry for induction of fluorescence 48 hours after temozolomide treatment, with the clone exhibiting the greatest induced fluorescence designated U87/pGADD34-EGFP. Clones from the pCDNA3-MGMT transfection were screened for temozolomide sensitivity. The clone that was most temozolomide resistant was screened for MGMT messenger ribonucleic acid (mRNA) levels by real time reverse-transcriptase polymerase chain reaction (RT-PCR), and was designated U87/MGMT. Human astrocytes were obtained from ScienCell

(San Diego, CA) and cultured in human astrocyte medium (ScienCell).

Viruses

Wild-type HSV-1 strain F (obtained from B. Roizman, University of Chicago, Chicago, IL), strain F-derived γ 34.5⁻ ICP6⁻LacZ⁺ G207,³ strain F-derived γ 34.5⁻ R3616 (provided by B. Roizman),²⁴ wild-type HSV-1 strain KOS (obtained from D. Knipe, Harvard Medical School, Boston, MA), and KOS-derived ICP6⁻LacZ⁺ hrR3 (obtained from S. Weller; University of Connecticut, Farmington, CT)²⁵ were grown, purified, and titered by plaque assay on Vero cells, as described.³

Cell Culture Cytotoxicity and Chou-Talalay Analysis

Temozolomide (Schering-Plough; Kenilworth, NJ) was dissolved in saline, cisplatin (Sigma, St. Louis, MO) was dissolved in dimethylsulfoxide (DMSO), and MGMT inhibitor O6BG (Sigma) was dissolved in distilled water. U87, T98, U87/MGMT, or human astrocytes were incubated overnight in 96-well plates (4000 cells/well). The next day, virus and/or chemotherapy were added to cells. Temozolomide was sometimes supplemented with 100 μ mol/L O6BG. Cells were incubated for 4 days. Survival was assessed using the 3-[4,5-dimethylthiazol-2-yl]-2,5-diphenyl-2H-tetrazolium bromide (MTT) assay (Sigma) according to the manufacturer's protocol. Dose-response curves were fit to Chou-Talalay lines,²² derived from the law of mass action, and described by the equation: $\log(fa/fu) = m \log D - m \log D_m$, where fa is the fraction affected (percent cell death), fu is the fraction unaffected (percent cell survival), D is the dose, D_m is the median-effect dose (dose causing 50% of cells to be affected, i.e., 50% survival), and m is the coefficient signifying the dose-response curve shape. Chemotherapy and virus were then added in combinations in a ratio equaling the ratio of their D_m s. After fitting the combined dose-response curve to a Chou-Talalay line, Chou-Talalay combination indices (CIs) were calculated for each fa using the equation $CI = [(D1/DX1) + (D2/DX2) + (D1)(D2)] / [(DX1)(DX2)]$, where $DX1$ and $DX2$ are the chemotherapy and virus doses required to achieve a particular fa , and $D1$ and $D2$ are the doses of the two combined required to achieve the same fa . Levels of interaction are defined as follows: CI greater than 1.3 indicates antagonism, CI between 1.1 and 1.3 indicates moderate antagonism, CI between 0.9 and 1.1 indicates additivity, CI between 0.8 and 0.9 indicates slight synergy, CI between 0.6 and 0.8 indicates moderate synergy, CI between 0.4 and 0.6 indicates synergy, and CI less than 0.4 indicates strong synergy.²⁶

Single-Step Growth Curves

U87 cells were plated at 2.5×10^5 cells/well into 12-well plates containing no drug, 300 $\mu\text{mol/L}$ temozolomide, or 0.1 $\mu\text{mol/L}$ cisplatin for 24 hours. These concentrations are nontoxic to U87 when treatment is for 72 hours. Cells were then infected with G207 at a multiplicity of infection (MOI) of 1.5 in the presence or absence of the same temozolomide or cisplatin concentrations. Cells were scraped into the medium and subjected to three freeze-thaw cycles at various time points up to 48 hours after infection. Virus titers were determined by plaque assays on Vero cells.

Quantitative Real-Time RT-PCR

U87, T98, U87/MGMT, or human astrocyte cells were treated for 48 hours with 10 $\mu\text{mol/L}$ to 3 mmol/L temozolomide or 0.01–1 $\mu\text{mol/L}$ cisplatin. These doses give 30 to 90% survival after 4 days, but 100% survival at 24 to 48 hours. RNA was extracted from cells with Trizol (Invitrogen). A high-capacity cDNA archive kit (Applied Biosystems, Foster City, CA) was used to generate cDNA. Real-time RT-PCR was performed on an ABI Prism 7000 (Applied Biosystems) machine using previously described human GADD34,²⁰ MGMT,²⁷ ATM,²⁸ ATR,²⁹ MPG,³⁰ and PADPRP¹² primers (Invitrogen) combined with SYBR Green Master Mix (Applied Biosystems) or primer-probe combinations for RR subunits M1 and M2 (Applied Biosystems) and 18S ribosomal RNA (rRNA) (Applied Biosystems) combined with TaqMan Master Mix (Applied Biosystems). Relative quantification was performed using 18S rRNA as an endogenous control. All reactions began with 10 minutes at 95°C for AmpliTaq Gold activation, followed by 40 cycles at 95°C for 15 seconds for denaturation, then 60°C for 1 minute for annealing/extension.

Small Interfering RNA

To silence gene expression, duplex RNA targeting human GADD34,²⁰ the M2 subunit of human RR,³¹ and control small interfering RNA (siRNA) with medium GC content (comparable to the other siRNAs used) targeting no vertebrate sequences were synthesized with d(TT) at the 3' terminus of each strand (Invitrogen). siRNA was transfected into U87 or T98 cells using Lipofectamine 2000 according to the manufacturer's protocol (Invitrogen). Levels of GADD34 and RR M2 subunit mRNA relative to mock-transfected cells were assessed at 24, 48, and 72 hours after transfection using real time RT-PCR and were reduced to 27 to 30%, 3 to 7%, and 25 to 28% of baseline values, respectively. Control siRNA maintained GADD34 and RR MR subunit mRNA levels at 95 to 100% of nontransfected cells 24 to 72 hours after transfection. Knockdown of protein levels by siRNA was confirmed by Western blot analysis. Total protein from cultured cells was extracted by RIPA buffer and 30 μg of protein was

separated on a 8% sodium dodecylsulfate (SDS)-polyacrylamide gel electrophoresis (PAGE) gel, transferred to polyvinylidene fluoride (PVDF) membrane, and incubated with antibodies to GADD34 (Imgenex Corp., San Diego, CA) or RR M2 subunit (GenWay Biotech, San Diego, CA) at 4°C overnight. Membranes were then incubated with peroxidase-conjugated secondary antibodies for 40 minutes the next day. Protein was visualized using the enhanced chemiluminescence kit (Amersham Biosciences, Piscataway, NJ).

Alkaline Comet Assay

Temozolomide-induced DNA damage was quantified using the alkaline comet assay. Cells were treated with varying temozolomide concentrations for 6 hours, suspended in low-melt agarose (Trevigen, Inc., Gaithersburg, MD), and placed onto comet slides (Trevigen). After the agarose solidified, the slides underwent lysis and electrophoresis according to the manufacturers' protocol for the alkaline comet assay. After labeling nuclei with SYBR green dye according to protocol, slides were photographed using confocal microscopy, and tail moments of 50 cells per slide were calculated using CometScore software (TriTek Corporation, Sumerduck, VA).

Flow Cytometry

U87/pGADD34-EGFP cells were treated for 48 hours with varying temozolomide concentrations. Apoptosis was screened for using the Annexin V-PE Apoptosis Detection Kit (BD Biosciences, San Jose, CA). A BD FACSCalibur Flow Cytometer (BD Biosciences) was used to sort cells on the basis of phycoerythrin (PE), EGFP, and 7-amino-actinomycin D (7-AAD) positivity, with 7-AAD positive cells (dead cells) gated out of any subsequent analysis. To assess viral replication in GADD34-expressing cells, temozolomide-treated U87/pGADD34-EGFP cells were sorted on the basis of EGFP expression using a BD FACS Vantage SE Flow Cytometer (BD Biosciences). EGFP⁺ and EGFP⁻ cells were then infected with G207 (MOI, 1.5), with viral yield determined as described above.

Immunohistochemistry

U87/pGADD34-EGFP cells were treated for 48 hours with 100 $\mu\text{mol/L}$ temozolomide, followed by infection with G207 (MOI, 0.1) for 10 hours. Cells were then fixed in 4% paraformaldehyde, stained with mouse anti- β -galactosidase (Promega, Madison, WI), stained with Texas Red-conjugated sheep anti-mouse antibody (Amersham), and mounted and counterstained with Vectashield mounting medium with diamidino phenyl indole (DAPI) nuclear stain (Vector Laboratories, Burlingame, CA).

In Vivo Experiments

Athymic mice (20 g) were inoculated subcutaneously with 10^6 U87 cells. Two weeks later, mice with 12 to 36 mm³

tumors were placed into treatment groups (five mice per treatment group), each with the same mean tumor volume. Mice were treated with 100 mg/kg/d temozolomide intraperitoneally for 14 days, the maximum tolerated temozolomide dose, and/or 5×10^6 pfu (plaque-forming units) G207 intratumorally in 30 μ L on treatment days 2 and 5. Mock-treated mice received equivalent intraperitoneal or intratumoral volumes of saline. Tumors were measured biweekly using calipers to calculate length, width, and height, with the measurer blinded to each animal's treatment group. Tumor volume was the product of these dimensions, and fold-growth was relative to treatment day 1. Measurement of a mouse's tumor continued until the mouse had to be killed because of excessive tumor (2.1 cm maximal dimension).

To assess viral replication in subcutaneous tumors, 20 days after subcutaneous inoculation of 10^6 U87 cells into athymic mice, when tumors had achieved volumes of 80 to 120 mm³, mice were treated intraperitoneally with saline (n = 20) or with 100 mg/kg/d temozolomide (n = 20). On the third treatment day, 5×10^6 pfu G207 was inoculated intratumorally into each tumor. Animals were killed and tumors excised at 2, 4, 6, and 8 days after G207 inoculation (five mice per group per time point), with temozolomide treatment continuing until the time of killing. Tumors were weighed, cut into small pieces, suspended in a volume of phosphate-buffered saline (PBS) that was twice the tumor volume, homogenized manually, sonicated, and centrifuged. The supernatant was isolated, freeze-thawed three times, and titered on Vero cells.

For intracranial studies, athymic mice (10 mice per treatment group) were anesthetized with intraperitoneal injection of 75 mg/kg ketamine and 15 mg/kg xylazine. After making a midline sagittal incision in mice immobilized in a stereotactic apparatus, a 1-mm burr hole was drilled 1 mm anterior to and 2.5 mm right of the bregma. Two hundred thousand U87 cells in 2 μ L were then injected 4.5 mm deep, using a Hamilton syringe. On days 7, 8, and 9 after injecting tumor cells, mice were treated with 100 mg/kg intraperitoneal temozolomide or saline. On day 10, mice were treated with 7×10^5 pfu G207 in 2 μ L of saline using the same burr hole at which tumor cells were injected. Intracranial tumor was confirmed postmortem in all mice that died. The MGH Subcommittee on Research Animal Care approved all animal protocols.

Statistical Analysis

Comparisons of variables (in vitro and in vivo viral yield, mean tail moment, percent apoptosis, percent of cells that were positive for β -galactosidase, and fold-growth of subcutaneous tumors) were made using a two-tailed Student's *t* test. Comparisons of Kaplan-Meier curves were made using the log-rank test.

RESULTS

Treatment of p53-Intact MGMT-Negative Glioma Cells with Oncolytic HSV and Chemotherapy

For MGMT-negative p53 wild-type cultured U87 human glioma cells,³² Dm of 390 μ mol/L temozolomide or 0.08 MOI G207 were reduced 100-fold by combined treatment (Dm, 3.9 μ mol/L temozolomide; 0.0008 MOI G207), with Chou-Talalay combination indices (CI quantifies the relationship between individual versus combined doses required for a particular fraction cell death, fa) below 0.009, well below the 0.4 cutoff for strong synergy (Fig. 9.1).

To determine whether strong synergy was unique to the temozolomide plus G207 combination, cisplatin, another glioma chemotherapy, was combined with HSV. Cisplatin, an

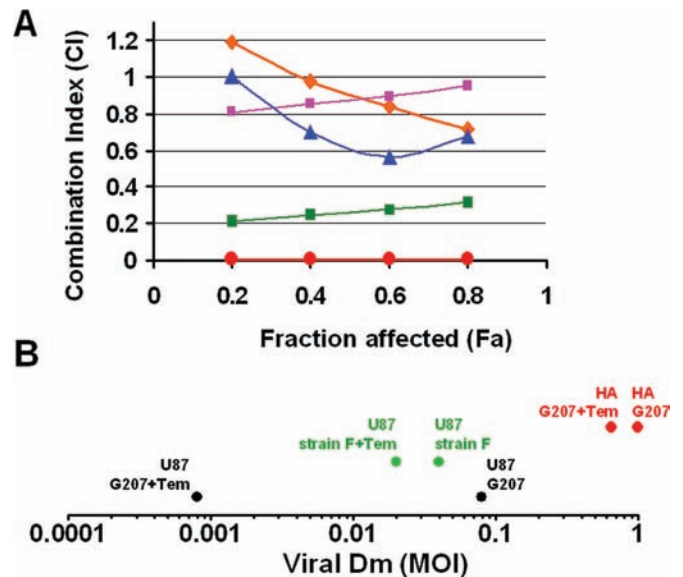


FIGURE 9.1. Interaction between HSV and temozolomide in MGMT-negative cells. **A**, Chou-Talalay analysis of U87 cells treated with temozolomide and wild-type HSV (strain F or KOS) or mutated oncolytic HSV (R3616, hrR3, or G207). CI is plotted as a function of fa. CI greater than 1.3 indicates antagonism, CI between 1.1 and 1.3 indicates moderate antagonism, CI between 0.9 and 1.1 indicates additivity, CI between 0.8 and 0.9 indicates slight synergy, CI between 0.6 and 0.8 indicates moderate synergy, CI between 0.4 and 0.6 indicates synergy, and CI less than 0.4 indicates strong synergy. **(B)** Dm of HSVs without or with temozolomide (*Tem*) in treating U87 glioma cells or human astrocytes (*HA*). Because of additivity or antagonism, wild-type HSV strain F in treating U87 and G207 in treating *HA* experienced minimal decreases in their Dm, whereas strong synergy caused a 100-fold decrease in the Dm of G207 in treating U87. This meant that temozolomide caused G207 to be more potent than wild-type strain F and widened the therapeutic window of doses in which G207 could lyse U87 cells without affecting human astrocytes.

TABLE 9.1. Interactions between chemotherapy and oncolytic HSV in various glioma cell lines^a

Cell line and chemotherapy agent	Dm drug alone	Range of CI values for chemotherapy plus virus				
		G207	R3616	hrR3	Strain F	KOS
Temozolomide						
U87	390 μmol/L	0.005–0.009 ^b	0.21–0.32 ^b	0.56–1.01	0.72–1.19	0.81–0.95
U373	250 μmol/L	0.03–0.1 ^b	ND	ND	ND	ND
T98	1844 μmol/L	0.96–1.23	1.04–1.32	0.62–5.66	ND	ND
T98 + O6BG	100 μmol/L	0.12–0.32 ^b	0.74–4.80	0.06–0.38 ^b	ND	ND
U87/mp53	800 μmol/L	0.55–0.90	0.72–1.02	0.77–1.12	ND	ND
U87/mp53 + O6BG	370 μmol/L	0.17–0.36 ^b	0.69–0.93	0.19–0.34 ^b	ND	ND
U87/MGMT	1807 μmol/L	0.74–0.78	0.78–1.48	0.54–0.87	ND	ND
U87/MGMT + O6BG	360 μmol/L	0.16–0.39 ^b	0.84–1.43	0.15–0.22 ^b	ND	ND
U87 + GADD34siRNA	260 μmol/L	0.79–0.85	ND	ND	ND	ND
U87 + RRsiRNA	370 μmol/L	0.007–0.009 ^b	ND	ND	ND	ND
U87/MGMT + O6BG + GADD34siRNA	365 μmol/L	0.02–0.05 ^b	ND	ND	ND	ND
U87/MGMT + O6BG + RRsiRNA	260 μmol/L	0.81–0.89	ND	ND	ND	ND
Human Astrocytes	4784 μmol/L	1.22–2.17	ND	ND	ND	ND
Cisplatin						
U87	0.9 μmol/L	0.43–0.59	ND	ND	ND	ND
T98	9.6 μmol/L	0.54–1.92	ND	ND	ND	ND

^aInteraction was measured by CI values derived from Chou-Talalay analysis. CI > 1.3 indicates antagonism, CI = 1.1–1.3 indicates moderate antagonism, CI = 0.9–1.1 indicates additivity, CI = 0.8–0.9 indicates slight synergy, CI = 0.6–0.8 indicates moderate synergy, CI = 0.4–0.6 indicates synergy, and CI < 0.4 (these combinations are marked ^b) indicates strong synergy. Each combination was studied in three independent experiments, the results of which had no statistically significant difference. The results of single experiments are shown above. ND, not determined.

intercalating agent, disrupts DNA replication and/or transcription, via a different mechanism than temozolomide. Treating U87 with G207 and cisplatin demonstrated much lesser effects (CI, 0.43–0.59; *Table 9.1*).

To determine whether G207 mutations contributed to the strong synergy between temozolomide and G207, we treated U87 with temozolomide combined with γ 34.5-deleted HSV R3616 or ICP6-mutated hrR3, or their respective wild-type parental HSV-1 strains, F and KOS. Strong synergy occurred when treating U87 with R3616 and temozolomide (CI, 0.21–0.32; *Fig. 9.1A*), virtually no synergy occurred when treating U87 with hrR3 and temozolomide (CI, 0.56–1.01; *Fig. 9.1A*), and no synergy occurred when treating U87 with temozolomide and strain F or KOS (CI, 0.72–1.19; *Fig. 9.1A*). Lack of synergy with other viruses does not reflect greater replication proficiency, because Chou-Talalay analysis adjusts doses to achieve comparable effects. The Dm of G207 on U87 (MOI 0.08) exceeded that of strain F without temozolomide (MOI 0.04), but became considerably lower than that of strain F with temozolomide (when combined with temozolomide: Dm G207 = MOI 0.0008; Dm strain F = MOI 0.02), indicating that temozolomide made G207 more potent than wild-type HSV (*Fig. 9.1B*).

In contrast, cultured human astrocytes exhibited minimal temozolomide (Dm = 4784 μmol/L) or G207 (Dm = 0.99 MOI) sensitivity, and temozolomide and G207 were antagonistic when treating astrocytes (*Table 9.1*).

Effect of Glioma p53 Mutations and MGMT Expression on the Interaction of Temozolomide with Oncolytic HSV

In contrast to U87 cells, T98 human glioma cells are temozolomide resistant, because of MGMT expression,^{16,32,33} and p53 mutated. Treating cultured T98 with G207, R3616, or hrR3 combined with temozolomide caused mostly additive (R3616, G207) or antagonistic (hrR3) interactions, with a CI of 0.62 to 5.66 (*Fig. 9.2A*). However, after adding the MGMT inhibitor, O6BG, synergy existed between temozolomide and G207 or hrR3 (CI, 0.06–0.38), but not between temozolomide and R3616 (*Fig. 9.2B*; CI, 0.74–4.80).

The role of p53 mutations in the interaction of temozolomide with recombinant HSV was explored using U373, a p53-mutated MGMT-negative human glioma cell line.³² Temozolomide and G207 were strongly synergistic when treating U373 (*Table 9.1*).

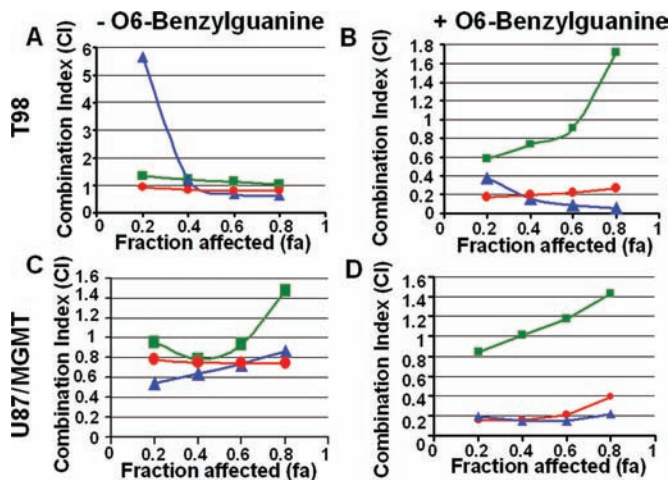


FIGURE 9.2. Interaction between HSV and temozolomide in MGMT-expressing cells. Chou-Talalay analysis of T98 (A, B) or U87/MGMT (C, D) human glioblastoma cells treated with temozolomide and mutated oncolytic HSV (R3616, hrR3, or G207) in the absence (A, C) or presence (B, D) of O6BG. CI is plotted as a function of fa. CI greater than 1.3 indicates antagonism, CI between 1.1 and 1.3 indicates moderate antagonism, CI between 0.9 and 1.1 indicates additivity, CI between 0.8 and 0.9 indicates slight synergy, CI between 0.6 and 0.8 indicates moderate synergy, CI between 0.4 and 0.6 indicates synergy, and CI less than 0.4 indicates strong synergy.

We then studied U87/mp53, a transfectant expressing mutant p53. U87/mp53 had twice the temozolomide Dm of U87 (Table 9.1). Real time RT-PCR revealed that all U87-derived p53-mutated clones, including U87/mp53, had twice as much MGMT mRNA as U87, suggesting that the U87/mp53 p53 mutation increased MGMT expression, which reduced temozolomide sensitivity. U87/mp53 generated similar interactions between temozolomide and oncolytic HSV as T98 (Table 9.1).

To isolate the role of MGMT from p53 status, we investigated U87/MGMT, a transfectant retaining the wild-type p53 of U87, but possessing 8-fold more MGMT mRNA than U87 (comparable to the 11-fold more MGMT mRNA in T98 than U87), increasing the temozolomide Dm 4.6-fold (Table 9.1). U87/MGMT generated similar interactions between temozolomide and oncolytic HSV as T98: virtually no synergy between temozolomide and any HSV (CI, 0.54–1.48; Fig. 9.2C) until O6BG treatment, which caused strong synergy between temozolomide and G207 or hrR3 (CI, 0.15–0.39) and additivity/antagonism between temozolomide and R3616 (CI, 0.84–1.43; Fig. 9.2D).

Therefore, O6BG-treated MGMT-expressing tumors exhibited synergy between temozolomide and RR⁻ viruses regardless of p53 status. Although p53 mutations in T98 (codon 237) and U87/mp53 (codon 143), in multiple clones, were associated with MGMT expression, the U373 p53

mutation (codon 273) was not associated with MGMT expression.

Increased G207 Yield from Temozolomide-Treated Infected Cells In Vitro and In Vivo

To determine whether synergy resulted from temozolomide enhancing G207 replication in U87, the effect of chemotherapy on infectious G207 yield was determined in single-step growth experiments. By 48 hours after infection, temozolomide-treated cells yielded greater than fivefold more G207 than untreated or cisplatin-treated cells ($P = 0.005$; Fig. 9.3A). Similarly, 2 to 8 days after G207 infection of subcutaneous U87 tumors in athymic mice, tumors from mice pretreated with temozolomide produced sixfold more G207 than those treated with saline ($P < 0.01$; Fig. 9.3B).

Temozolomide-Induced DNA Repair Genes Vary with MGMT Expression

Next, we investigated whether U87 temozolomide treatment enhanced G207 replication because of temozolomide-induced DNA repair genes, and whether the different

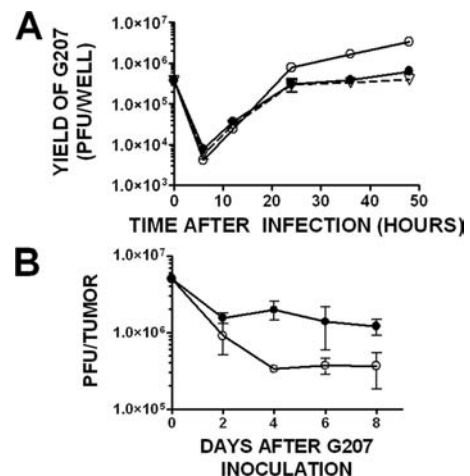


FIGURE 9.3. Effect of chemotherapy on G207 growth in U87 cells in culture and in vivo. A, single-step growth curve of G207 on U87 cells, which were pretreated for 24 hours with 300 $\mu\text{mol/L}$ temozolomide or 0.1 $\mu\text{mol/L}$ cisplatin, followed by infection with G207 at an MOI of 1.5. At the indicated times after infection, virus was isolated from cells (plated in triplicate) and titers determined. Shown are titers (pfu recovered per infected well, with standard deviations) at multiple times up to 48 hours after infection for cells treated with no drug, temozolomide, or cisplatin. Cisplatin curve did not differ statistically from non-drug treated ($P 0.05$), whereas temozolomide-treated cells produced more virus from 24 to 48 hours after infection ($P < 0.006$). B, titers of G207 harvested from excised subcutaneous U87 tumors in athymic mice at 2, 4, 6, and 8 days after G207 inoculation in mice pretreated for 3 days with 100 mg/kg/d temozolomide or saline. There was significantly more G207 recovered from temozolomide-treated tumors than from saline-treated tumors at all times evaluated ($P < 0.01$ at all time points). Standard deviations are shown.

interactions between temozolomide and HSV mutants observed in MGMT-expressing cells reflected induction of different DNA repair genes. Using real-time RT-PCR, we investigated genes contributing to repair of temozolomide-induced DNA damage, some of which enhance HSV replication: MPG, PADPRP, ATR, and ATM.^{12,13,34} We also investigated GADD34 and RR, genes complementing specific HSV mutations and possibly assisting the cellular DNA damage response. Treating U87 cells with 1 mmol/L temozolomide for 48 hours increased GADD34 expression 16-fold, exceeding the effects on other assessed transcripts (Fig. 9.4A; Table 9.2). Treating U87 cells with 1 μ mol/L cisplatin did not significantly increase assessed transcript expression. No assessed transcripts increased after temozolomide treatment of human astrocytes, T98, U87/MGMT, or U87/mp53 (Fig. 9.4A; Table 9.2). Treating T98, U87/MGMT, or U87/mp53 with 1 mmol/L temozolomide and 100 μ mol/L O6BG increased RR M2 subunit expression 9- to 15-fold, exceeding the effects on other assessed transcripts (Fig. 9.4A; Table 9.2). Temozolomide-induced GADD34 and RR M2 subunit protein expression in U87 and O6BG-treated T98, along with siRNA-mediated inhibited protein expression, were confirmed by Western blots (Fig. 9.4B).

GADD34 and RR Contribute to DNA Repair and Synergy

Because they were the most temozolomide-induced transcripts assessed, we investigated whether GADD34 and RR assist repair of temozolomide-induced DNA damage. The alkaline comet assay was used to measure temozolomide-induced single-strand breaks. The mean tail moment, reflecting cumulative DNA damage, of U87 cells treated for 6 hours with temozolomide varied with temozolomide concentration, whereas, in U87/MGMT, it was minimal regardless of temozolomide dose (Fig. 9.4C). O6BG-treated U87/MGMT exhibited the same increase in tail moment with temozolomide concentration seen in U87 (Fig. 9.4C). RR siRNA, which targets RR M2 subunit mRNA, and GADD34 siRNA did not alter the tail moments at multiple temozolomide concentrations in U87 and O6BG-treated U87/MGMT, respectively. Adding GADD34 siRNA to U87 cells or RR siRNA to O6BG-treated U87/MGMT cells increased the tail moment at each temozolomide concentration ($P < 0.005$), suggesting that GADD34 and RR prevented DNA damage accumulation, possibly by DNA repair. In addition, GADD34 and RR siRNA inhibited the synergy of G207 and temozolomide in U87 and O6BG-treated U87/MGMT cells, respectively (Table 9.1).

GADD34 Is Expressed Mostly in Nonapoptotic Cells after Temozolomide Treatment

Speculated GADD34 roles include DNA repair or apoptosis.⁵ Our hypothesis that temozolomide-induced

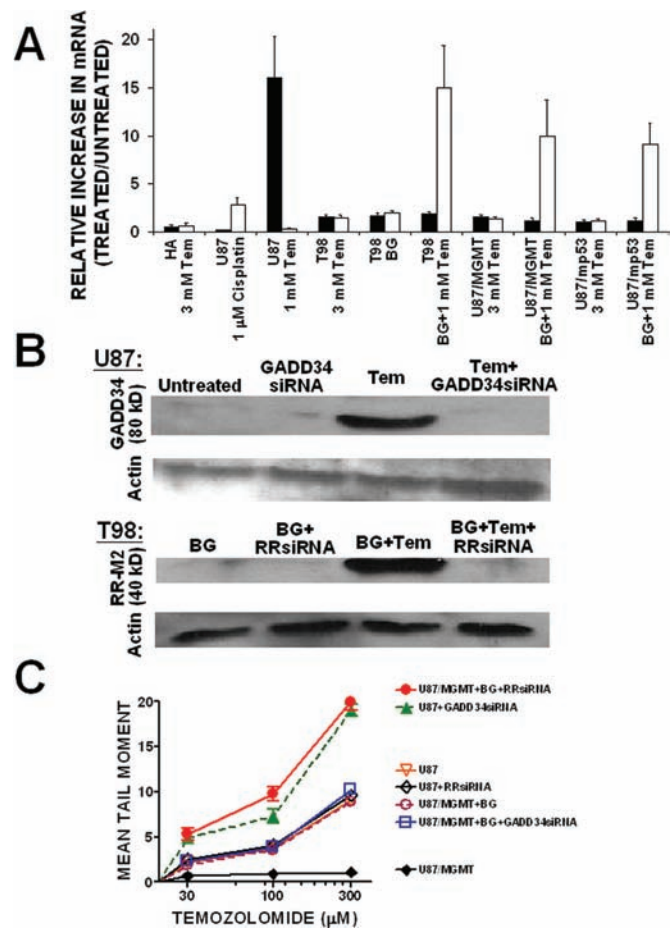


FIGURE 9.4. Effect of temozolomide on GADD34 and RR mRNA and protein; contribution of GADD34 and RR to DNA repair. *A*, results of real time RT-PCR analysis of levels of mRNA encoding GADD34 and the M2 subunit of RR in drug-treated human astrocyte (HA), U87, T98, U87/MGMT, and U87/mp53 cells. Cells were treated for 48 hours with varying concentrations of temozolomide (Tem), cisplatin, or O6BG. Values shown are relative amounts of mRNA for GADD34 (black) and the M2 subunit of RR (white) compared with untreated cells. Standard deviations are shown. *B*, Western blot analysis of: 1, GADD34 expression in U87 cells that were untreated, treated with GADD34 siRNA, treated with 1 mmol/L temozolomide, and treated with temozolomide plus GADD34 siRNA; and 2, RR M2 subunit expression in T98 cells that were treated with 100 μ mol/L O6BG, O6BG + RR siRNA, O6BG + 1 mmol/L temozolomide, and O6BG + 1 mmol/L temozolomide + RR siRNA. *C*, results of alkaline comet assay presented as mean tail moment as a function of temozolomide concentration for U87 cells treated with RR or GADD34 siRNA and U87/MGMT cells treated with O6BG (BG) plus RR or GADD34 siRNA. Standard deviations are shown in (A) and (C).

GADD34 expression enhanced G207 replication could only explain the observed synergy if GADD34 expression was not limited to cells undergoing apoptosis after temozolomide treatment, because enhanced viral replication in such cells

TABLE 9.2. Induction of genes in U87 cells, U87/MGMT cells, and human astrocytes treated for 48 hours with temozolomide, temozolomide plus O6BG, or cisplatin^a

Gene	U87 1 mmol/L temozolomide			U87/MGMT 1 mmol/L temozolomide + 100 μmol/L O6BG			U87 1 μmol/L cisplatin			Human Astrocytes 3 mmol/L temozolomide		
	-ΔΔC _T	Fold-induction (2 ^{-ΔΔC_T})	-ΔΔC _T	Fold-induction (2 ^{-ΔΔC_T})	-ΔΔC _T	Fold-induction (2 ^{-ΔΔC_T})	-ΔΔC _T	Fold-induction (2 ^{-ΔΔC_T})	-ΔΔC _T	Fold-induction (2 ^{-ΔΔC_T})	-ΔΔC _T	Fold-induction (2 ^{-ΔΔC_T})
ATM	-1.81 ± 0.73	0.29 (0.17-0.47)	-0.37 ± 0.30	0.77 (0.63-0.95)	-2.89 ± 0.91	0.13 (0.07-0.25)	-0.59 ± 0.40	0.67 (0.50-0.88)				
ATR	0.32 ± 0.18	1.25 (1.10-1.41)	0.76 ± 0.40	1.69 (1.28-2.23)	-2.21 ± 0.90	0.22 (0.12-0.40)	-2.0 ± 1.9	0.25 (0.07-0.93)				
GADD34	4.0 ± 0.31	16.0* (12.9-19.8)	0.30 ± 0.19	1.23 (1.13-1.40)	-2.60 ± 0.30	0.16 (0.13-0.20)	-0.80 ± 0.24	0.57 (0.49-0.68)				
MPG	1.41 ± 0.39	2.66 (2.03-3.48)	1.46 ± 0.44	2.76 (2.03-3.73)	-0.80 ± 0.65	0.80 (0.37-0.90)	-0.46 ± 0.80	0.72 (0.42-1.30)				
PADPRP	1.1 ± 0.53	2.14 (1.48-3.10)	1.0 ± 0.42	2.0 (1.49-2.68)	-2.44 ± 2.0	0.18 (0.05-0.74)	-2.0 ± 1.6	0.25 (0.08-0.76)				
RR M1	-1.5 ± 0.32	0.35 (0.28-0.44)	-1.7 ± 1.1	0.31 (0.14-0.66)	1.50 ± 0.30	2.83 (2.30-3.48)	1.1 ± 0.38	2.14 (1.65-2.79)				
RR M2	-1.9 ± 0.51	0.27 (0.19-0.38)	3.3 ± 0.43	9.85* (7.31-13.27)	1.50 ± 0.30	2.83 (2.30-3.48)	-0.60 ± 0.24	0.66 (0.48-0.90)				

^aReal-time RT-PCR was used to determine -ΔΔC_T = -(C_T mRNA of interest drug treated - C_T 18S rRNA of interest untreated - C_T 18S rRNA untreated), which enabled determination of fold-induction (2^{-ΔΔC_T}) in treated cells relative to untreated cells. C_T, cycle threshold. Experiments were performed three separate times, each time in triplicate. The -ΔΔC_T values given are averages from a single experiment followed by standard deviations, and the fold-induction given is derived from the mean -ΔΔC_T followed by lower and upper limits, which are derived from mean -ΔΔC_T ± one standard deviation of -ΔΔC_T.

*Significant inductions (more than threefold).

would not augment cytotoxicity. Therefore, we investigated which cells express GADD34 after temozolomide treatment via U87/pGADD34-EGFP cells, in which the human GADD34 promoter drives EGFP expression, causing green fluorescence after temozolomide treatment (Fig. 9.5A). fluorescent activated cell sorting (FACS) analysis identified 2- to 2.5-fold more apoptosis in EGFP-negative live cells than in EGFP-positive live cells (P < 0.002), suggesting more-frequent GADD34 expression in cells that were going to survive temozolomide treatment (Fig. 9.5B-C).

Enhanced G207 Replication in GADD34-Expressing Tumor Cells

To determine whether G207 protein expression was enhanced in tumor cells expressing GADD34 after temozolomide treatment, U87/pGADD34-EGFP cells treated with 100 μmol/L temozolomide for 48 hours followed by G207 infection (MOI = 0.1) for 10 hours were stained with an antibody to G207-expressed marker protein β-galactosidase (Fig. 9.5D). β-galactosidase expression was fourfold more frequent in EGFP⁺ than EGFP⁻ cells (P = 0.001; Fig. 9.5E), suggesting greater G207 protein expression in cells expressing GADD34 after temozolomide treatment. To confirm whether G207 replicated more in tumor cells expressing GADD34 after temozolomide treatment, U87/pGADD34-EGFP cells treated with 100 μmol/L temozolomide for 48 hours were FACS-sorted for EGFP expression. EGFP⁺ and EGFP⁻ cells were then infected with G207 (MOI = 1.5) for 48 hours. The G207 yield was fourfold higher from EGFP⁺ than EGFP⁻ cells (P = 0.002; Fig. 9.5F).

Combined Treatment In Vivo

Because of their strong synergy in treating cultured U87 cells, G207 and temozolomide were combined to treat subcutaneous U87 tumors in athymic mice at doses that alone inhibited tumor growth less than 50% (Fig. 9.6A). Fifteen days after treatment began, tumors receiving combined treatment grew significantly less than saline- or single agent-treated tumors (P = 0.037-0.048 combined versus saline or single agent; P = 0.51 single agent versus saline), a difference that remained significant thereafter. Tumor growth in single-agent versus saline-treated mice did not become significantly different until 26 days after treatment began, the last day of comparison, at which point, tumors grew 63-fold (saline), 35- to 36-fold (G207/temozolomide alone), and 10-fold (G207+temozolomide) (P = 0.01-0.02 for single agent versus saline, P = 0.00009-0.001 for combined versus saline or single agent). Excessive tumor burden occurred at median times of 29 days (saline treatment), 40 days (single treatment), or 54 days (combined treatment) (P = 0.003 or 0.0025 for single versus combined or saline-treatment, respectively; P = 0.002 for combined versus saline treatment;

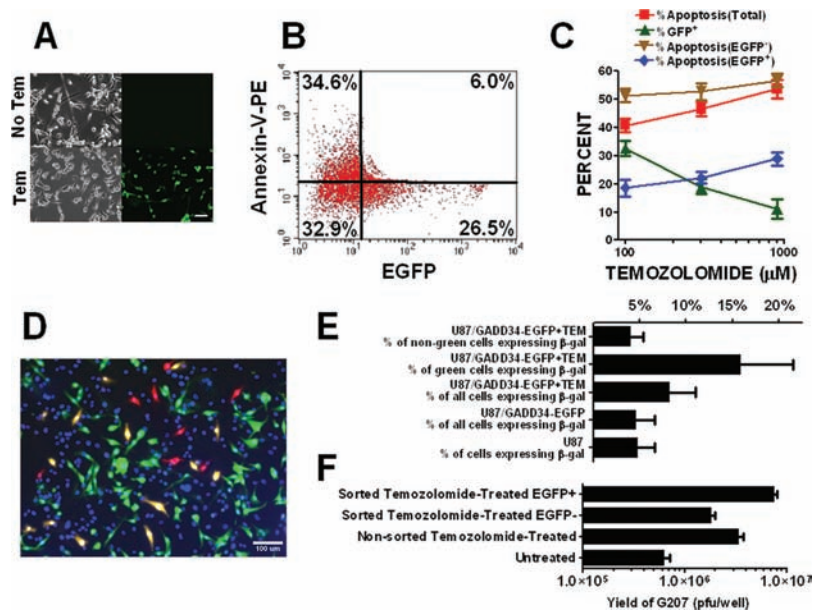


FIGURE 9.5. GADD34 expression is greater in nonapoptotic cells that survive temozolomide treatment, and G27 replication is enhanced in tumor cells expressing GADD34 after temozolomide treatment. *A*, U87/pGADD34-EGFP cells do not express EGFP (upper row) unless treated with temozolomide (lower row; 48 hours after treatment with 50 μmol/L temozolomide). In each set, left panel is a phase contrast image and right panel is a fluorescent image. Field shown is original magnification ×30. Scale bar represents 100 μm. *B*, assessment of apoptosis (as determined by Annexin V-PE staining) and EGFP expression by flow cytometry of U87/pGADD34-EGFP cells treated with 100 μmol/L temozolomide for 48 hours. *C*, percentage of 7-AAD negative cells that were apoptotic (%Apoptosis[Total]) or EGFP-positive (% GFP⁺) and percentage of EGFP-positive and EGFP-negative cells that were apoptotic after 48 hours of treating U87/pGADD34-EGFP cells with varying temozolomide concentrations (%Apoptosis[GFP⁺] and %Apoptosis[GFP⁻], respectively). Each concentration was studied in triplicate, and the experiment was repeated in triplicate, with results of a representative experiment, including standard deviations, shown. There was 2- to 2.5-times more apoptosis in EGFP-negative than in EGFP-positive cells at all temozolomide concentrations tested ($P < 0.0002$). *D*, U87/GADD34-EGFP cells were treated with 100 μmol/L temozolomide for 48 hours, after which, GADD34-expressing cells exhibit green fluorescence. Cells were then infected with G27 at MOI = 0.1 for 10 hours, after which infected cells were stained red by a β-galactosidase-specific antibody, and all cell nuclei were counterstained with DAPI. Field shown is original magnification ×30. Scale bar represents 100 μm. *E*, from six images taken per well and five wells of U87/GADD34-EGFP with and without temozolomide and U87 cells undergoing the experiment described in (*D*), cells were counted to determine percentage of nongreen (blue nuclear staining), green, and/or total cells expressing β-galactosidase (β-gal). Per well, 15.8% of green (GADD34-expressing) cells were found to be infected (red + green = yellow), greater than the 3.9% per well of non-GADD34-expressing (blue nuclear staining alone) cells that were infected (red) ($P = 0.001$). Standard deviations derived from data in multiple wells are shown. (*F*) U87/GADD34-EGFP cells treated with 100 μmol/L temozolomide for 48 hours were FACS-sorted based on EGFP expression. EGFP⁺ and EGFP⁻ cells were then infected with G27 (MOI = 1.5). Infectious G27 yield determined after 48 hours of infection was greater in EGFP⁺ than EGFP⁻ cells ($P = 0.002$).

Fig. 9.6B). $P = 0.003$ or 0.0025 for single versus combined or saline-treatment, respectively; $P = 0.002$ for combined versus saline treatment²⁷? Athymic mice bearing orthotopic intracranial U87 tumors treated with intraperitoneal temozolomide or intratumoral G27 achieved median survivals of 30.5 (saline) or 46 to 48 (G27/temozolomide alone) days. In contrast, temozolomide preceding G27 treatment caused 100% 90-day survival (*Fig. 9.6C*).

DISCUSSION

We hypothesized that mutations enabling cancer cells to express DNA repair genes after chemotherapy treatment could be used to improve oncolytic viral therapy. We, there-

fore, studied the effect of glioma MGMT expression on temozolomide-induced DNA repair genes, and whether these gene products increase replication of appropriately engineered oncolytic HSVs.

For cultured MGMT-negative U87 cells, synergy of γ34.5-deleted HSV with temozolomide was very strong, whereas combining G27 with cisplatin caused only moderate synergy. In contrast, cultured MGMT-expressing temozolomide-resistant cells showed no significant synergy when combining temozolomide with any HSV, but synergy between temozolomide and RR-mutated HSV arose after adding MGMT inhibitor, O6BG. The benefits of combined treatment were confirmed in vivo when athymic mice with

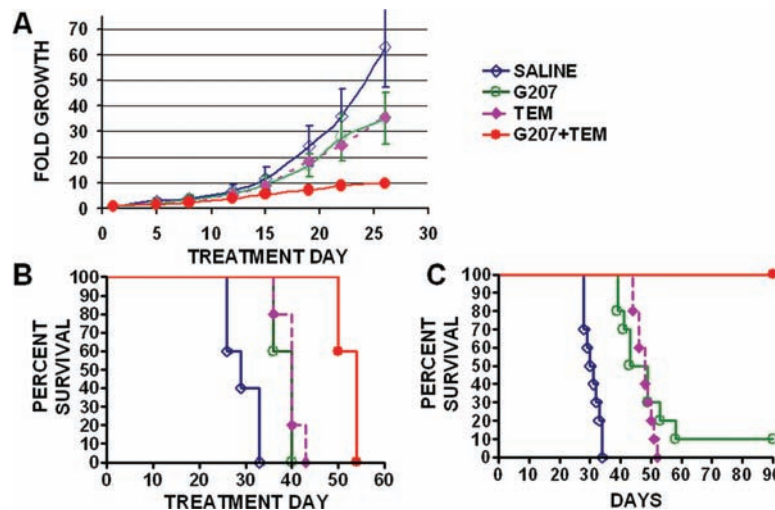


FIGURE 9.6. Treatment of U87 tumors in vivo. Results of treating subcutaneous (A, B) or orthotopic intracranial (C) U87 tumors in athymic mice with saline, temozolomide, G207, or temozolomide plus G207. Data is presented as fold-growth versus treatment day for subcutaneous tumors (A); as Kaplan-Meier curves documenting time until subcutaneous tumor size progressed to 2.1 cm in maximal dimension (B); or as Kaplan-Meier curves documenting survival of mice with intracranial U87 tumors (C). For subcutaneous tumors (A, B), there were five mice per treatment group and treatment was with 5×10^6 pfu G207 or saline administered intratumorally on treatment days 2 and 5 and 100 mg/kg/d temozolomide or saline administered intraperitoneally on treatment days 1 to 14. By 26 days after treatment began, subcutaneous tumors grew 63-fold (saline), 35-fold (G207), 36-fold (temozolomide), and 10-fold (G207 + temozolomide) ($P = 0.01$ – 0.02 single agent versus saline; $P = 0.00009$ – 0.001 combined versus saline or single agent). Standard deviations are shown. B, excessive subcutaneous tumor burden occurred at median times of 29 days (saline treatment), 40 days (single treatment), or 54 days (combined treatment) ($P = 0.003$ single versus combined, $P = 0.0025$ single versus saline treatment; $P = 0.002$ combined versus saline treatment). C, for intracranial tumors, there were 10 mice per treatment group and treatment was with 100 mg/kg temozolomide or saline intraperitoneally on days 7, 8, and 9 after tumor injection; or with 7×10^5 pfu G207 or saline administered intratumorally 10 days after tumor injection. Median survivals were 30.5 days (saline), 46 days (G207), and 48 days (temozolomide). In contrast, temozolomide preceding G207 treatment resulted in a 100% 90-day survival.

intracranial U87 tumors exhibited 100% long-term survival after treatment with G207 and temozolomide, compared with virtually none with either agent alone.

GADD34 and the RR M2 subunit were the most temozolomide-induced assessed transcripts in MGMT-negative and O6BG-treated MGMT-positive gliomas, respectively. Our findings suggest that GADD34 and RR reduce temozolomide-induced DNA damage in MGMT-negative and MGMT-positive gliomas, respectively, and enhance replication of $\gamma 34.5$ - and RR-mutated HSV viruses, respectively. Cisplatin, part of procarbazine-cisplatin-vincristine (PCV) glioma chemotherapy,³⁵ minimally induced the assessed transcripts, a likely explanation for the minimal synergy between cisplatin and G207. Thus, mutations enabling gliomas to express DNA repair genes after temozolomide treatment can be used to improve viral oncolysis, and a genetic alteration endowing gliomas with temozolomide resistance determines which genes temozolomide induces, which, in turn, determines the genetic profile of the oncolytic HSV whose replication temozolomide enhances.

DNA damage causes cells to initiate DNA repair and stop replicating. Although exact functions of the five known

GADD proteins remain unconfirmed, they are associated with apoptosis and cell cycle arrest,⁵ and are upregulated by some chemotherapies.^{20,21,36} RR synthesizes nucleotide precursors using homodimeric large (M1) and small (M2) subunits. M2 is upregulated during S-phase and by certain chemotherapies,³⁷ whereas M1 expression is constant during the cell cycle, diminishing only during G_0 arrest. This report furthers these demonstrations that certain chemotherapies induce GADD34 and RR by demonstrating that both proteins prevent accumulation of chemotherapy-induced DNA damage, possibly through DNA repair. In addition, our demonstration of GADD34 expression primarily in nonapoptotic cells surviving temozolomide treatment suggests greater G207 replication in cells surviving temozolomide treatment through DNA repair, underscoring the complementary tumoricidal effects of these two treatments, and unveiling the novel finding that oncolytic HSV can target tumor cells evading chemotherapy through DNA repair.

Our finding that chemotherapy-induced DNA repair genes enhanced replication of specific HSV mutants is consistent with reports of DNA repair enhancing HSV replication.³⁴ In contrast, DNA repair inhibits replication of adeno-

virus, another engineered oncolytic virus studied in clinical trials.^{34,38}

Although previous reports found that expressing wild-type p53 in p53-mutated gliomas reduces MGMT expression,³⁹ our finding that only certain p53 mutations increased MGMT expression suggests multifactorial MGMT regulation and that MGMT may not be upregulated in all of the 20% of glioblastomas with p53 mutations.⁴⁰ We found that MGMT expression determines temozolomide-induced DNA repair genes. Although one would expect O6BG-treated MGMT-expressing cells to accumulate and repair temozolomide-induced DNA damage similarly to MGMT-negative cells, previous reports demonstrated differences in the two scenarios, including temozolomide-induced apoptotic versus autophagic cell death in MGMT-negative versus O6BG-treated MGMT-positive cells, respectively.⁴¹ The different temozolomide-induced genes in these two scenarios suggests that the scenarios differ not just in cell death mechanism, but also in DNA repair mechanisms.

The 20% of gliomas expressing MGMT exhibit a 90% failure to respond rate to temozolomide, compared with the 40% failure rate of MGMT-negative gliomas.^{14,15} In phase I clinical trials, the MGMT-inhibitor O6BG enhanced the response of MGMT-expressing gliomas to temozolomide.¹⁶ Temozolomide induction of GADD34 in MGMT-negative cells and RR in O6BG-treated MGMT-positive cells suggests that constructs such as G207 may be ideal to combine with temozolomide because of synergy in both scenarios through induction of different complementary mammalian genes.

Dual G207 mutations increase safety, but sometimes reduce oncolysis compared with single mutated viruses.^{3,42} Because temozolomide causes strong synergy with specific HSVs through tumoral GADD34 or RR induction, but upregulates neither in astrocytes, antagonizing G207 replication, temozolomide enhances the potency and therapeutic window of G207. In fact, temozolomide increased G207 potency beyond that of its wild-type parental virus.

Glioma treatment with G207 and temozolomide also enhances temozolomide potency, reducing dosage and toxicity (e.g., myelosuppression). The temozolomide dose we used, the maximum tolerated murine dose (rodents exhibit slightly more temozolomide sensitivity than humans), was minimally effective alone. G207 also has a maximal in vivo dose, not from toxicity but from the large number of cells in a postsurgical glioma cavity; inefficient delivery and distribution; and viral titer limitations reflecting viral biology and production constraints. The synergy described here increases the efficacy of these lower viral MOIs.

Two suggestions emerge from the strong synergy found between specific engineered oncolytic HSVs and temozolomide. First, the concept of generating a drug-induced viral oncolysis-enhancing response selectively in tumor cells with specific mutations warrants further investigation. Second,

glioma treatment with temozolomide and G207, possibly giving temozolomide before inoculating virus during surgery to take advantage of temozolomide-induced DNA repair in residual glioma cells, warrants a clinical trial.

ACKNOWLEDGMENTS

We thank Drs. Roizman, Knipe, and Weller for providing virus. This work was supported in part by National Institutes of Health Grants NS32677 (to RLM) and P30 NS045776 (to SR) for the real-time PCR core. Robert Martuza and Samuel Rabkin are consultants to MediGene AG, which has a license from Georgetown University for G207.

REFERENCES

1. Bischoff JR, Kirn DH, Williams A, Heise C, Horn S, Muna M, et al.: An adenovirus mutant that replicates selectively in p53-deficient human tumor cells. *Science* 274(5286):373–376, 1996.
2. Coffey MC, Strong JE, Forsyth PA, Lee PW: Reovirus therapy of tumors with activated Ras pathway. *Science* 282(5392):1332–1334, 1998.
3. Mineta T, Rabkin SD, Yazaki T, Hunter WD, Martuza RL: Attenuated multi-mutated herpes simplex virus-1 for the treatment of malignant gliomas. *Nat Med* 1(9):938–943, 1995.
4. Stewart LA: Chemotherapy in adult high-grade glioma: A systematic review and meta-analysis of individual patient data from 12 randomised trials. *Lancet* 359(9311):1011–1018, 2002.
5. Liebermann DA, Hoffman B: Myeloid differentiation (MyD)/growth arrest DNA damage (GADD) genes in tumor suppression, immunity and inflammation. *Leukemia* 16(4):527–541, 2002.
6. Kolberg M, Strand KR, Graff P, Andersson KK: Structure, function, and mechanism of ribonucleotide reductases. *Biochim Biophys Acta* 1699(1–2):1–34, 2004.
7. He B, Chou J, Liebermann DA, Hoffman B, Roizman B: The carboxyl terminus of the murine MyD116 gene substitutes for the corresponding domain of the gamma(1)34.5 gene of herpes simplex virus to preclude the premature shutoff of total protein synthesis in infected human cells. *J Virol* 70(1):84–90, 1996.
8. Markert JM, Medlock MD, Rabkin SD, Gillespie GY, Todo T, Hunter WD, et al.: Conditionally replicating herpes simplex virus mutant, G207 for the treatment of malignant glioma: Results of a phase I trial. *Gene Ther* 7(10):867–874, 2000.
9. Kirn D, Martuza RL, Zwiebel J: Replication-selective virotherapy for cancer: Biological principles, risk management and future directions. *Nat Med* 7(7):781–787, 2001.
10. Chibbaro S, Benvenuti L, Caprio A, Carnesecchi S, Pulera F, Faggionato F, et al.: Temozolomide as first-line agent in treating high-grade gliomas: phase II study. *J Neurooncol* 67(1–2):77–81, 2004.
11. Denny BJ, Wheelhouse RT, Stevens MF, Tsang LL, Slack JA: NMR and molecular modeling investigation of the mechanism of activation of the antitumor drug temozolomide and its interaction with DNA. *Biochemistry* 33(31):9045–9051, 1994.
12. Tentori L, Turriziani M, Franco D, Serafino A, Levati L, Roy R, et al.: Treatment with temozolomide and poly(ADP-ribose) polymerase inhibitors induces early apoptosis and increases base excision repair gene transcripts in leukemic cells resistant to triazine compounds. *Leukemia* 13(6):901–909, 1999.
13. Caporali S, Falcinelli S, Starace G, Russo MT, Bonmassar E, Jiricny J, et al.: DNA damage induced by temozolomide signals to both ATM and ATR: role of the mismatch repair system. *Mol Pharmacol* 66(3):478–491, 2004.
14. Belanich M, Pastor M, Randall T, Guerra D, Kibitel J, Alas L, et al.: Retrospective study of the correlation between the DNA repair protein alkyltransferase and survival of brain tumor patients treated with carmustine. *Cancer Res* 56(4):783–788, 1996.
15. Friedman HS, McLendon RE, Kerby T, Dugan M, Bigner SH, Henry AJ, et al.: DNA mismatch repair and O6-alkylguanine-DNA alkyltransferase

- analysis and response to Temodal in newly diagnosed malignant glioma. **J Clin Oncol** 16(12):3851–3857, 1998.
16. Gerson SL: MGMT: Its role in cancer aetiology and cancer therapeutics. **Nat Rev Cancer** 4(4):296–307, 2004.
 17. Chahnavi A, Todo T, Martuza RL, Rabkin SD: Replication-competent herpes simplex virus vector G207 and cisplatin combination therapy for head and neck squamous cell carcinoma. **Neoplasia** 1(2):162–169, 1999.
 18. Cinatl J Jr, Cinatl J, Michaelis M, Kabickova H, Kotchetkov R, Vogel JU, et al.: Potent oncolytic activity of multimitated herpes simplex virus G207 in combination with vincristine against human rhabdomyosarcoma. **Cancer Res** 63(7):1508–1514, 2003.
 19. Toyozumi T, Mick R, Abbas AE, Kang EH, Kaiser LR, Molnar-Kimber KL: Combined therapy with chemotherapeutic agents and herpes simplex virus type 1 ICP34.5 mutant (HSV-1716) in human non-small cell lung cancer. **Hum Gene Ther** 10(18):3013–3029, 1999.
 20. Bennett JJ, Adusumilli P, Petrowsky H, Burt BM, Roberts G, Delman KA, et al.: Up-regulation of GADD34 mediates the synergistic anticancer activity of mitomycin C and a gamma134.5 deleted oncolytic herpes virus (G207). **Faseb J** 18(9):1001–1003, 2004.
 21. Petrowsky H, Roberts GD, Kooby DA, Burt BM, Bennett JJ, Delman KA, et al.: Functional interaction between fluorodeoxyuridine-induced cellular alterations and replication of a ribonucleotide reductase-negative herpes simplex virus. **J Virol** 75(15):7050–7058, 2001.
 22. Chou TC, Talalay P: Generalized equations for the analysis of inhibitions of Michaelis-Menten and higher-order kinetic systems with two or more mutually exclusive and nonexclusive inhibitors. **Eur J Biochem** 115(1):207–216, 1981.
 23. Baker SJ, Markowitz S, Fearon ER, Willson JK, Vogelstein B: Suppression of human colorectal carcinoma cell growth by wild-type p53. **Science** 249(4971):912–915, 1990.
 24. Chou J, Kern ER, Whitley RJ, Roizman B: Mapping of herpes simplex virus-1 neurovirulence to gamma 134.5, a gene nonessential for growth in culture. **Science** 250(4985):1262–1266, 1990.
 25. Goldstein DJ, Weller SK: Herpes simplex virus type 1-induced ribonucleotide reductase activity is dispensable for virus growth and DNA synthesis: Isolation and characterization of an ICP6 lacZ insertion mutant. **J Virol** 62(1):196–205, 1988.
 26. Chou TC, Talalay P: Quantitative analysis of dose-effect relationships: the combined effects of multiple drugs or enzyme inhibitors. **Adv Enzyme Regul** 22:27–55, 1984.
 27. Merlin JL, Marchal S, Ramacci C, Berlion M, Poullain MG: Enhancement of fotemustine (Muphoran) cytotoxicity by amifostine in malignant melanoma cell lines. **Anticancer Drugs** 13(2):141–147, 2002.
 28. Gilad S, Khosravi R, Harnik R, Ziv Y, Shkedy D, Galanty Y, et al.: Identification of ATM mutations using extended RT-PCR and restriction endonuclease fingerprinting, and elucidation of the repertoire of A-T mutations in Israel. **Hum Mutat** 11(1):69–75, 1998.
 29. Jones GG, Reaper PM, Pettitt AR, Sherrington PD: The ATR-p53 pathway is suppressed in noncycling normal and malignant lymphocytes. **Oncogene** 23(10):1911–1921, 2004.
 30. Kim NK, Ahn JY, Song J, Kim JK, Han JH, An HJ, et al.: Expression of the DNA repair enzyme, N-methylpurine-DNA glycosylase (MPG) in astrocytic tumors. **Anticancer Res** 23(2B):1417–1423, 2003.
 31. Duxbury MS, Ito H, Zinner MJ, Ashley SW, Whang EE: RNA interference targeting the M2 subunit of ribonucleotide reductase enhances pancreatic adenocarcinoma chemosensitivity to gemcitabine. **Oncogene** 23(8):1539–1548, 2004.
 32. Kanzawa T, Germano IM, Kondo Y, Ito H, Kyo S, Kondo S: Inhibition of telomerase activity in malignant glioma cells correlates with their sensitivity to temozolomide. **Br J Cancer** 89(5):922–929, 2003.
 33. Esteller M, Garcia-Foncillas J, Andion E, Goodman SN, Hidalgo OF, Vanaclocha V, et al.: Inactivation of the DNA-repair gene MGMT and the clinical response of gliomas to alkylating agents. **N Engl J Med** 343(19):1350–1354, 2000.
 34. Lilley CE, Carson CT, Muotri AR, Gage FH, Weitzman MD: DNA repair proteins affect the lifecycle of herpes simplex virus 1. **Proc Natl Acad Sci U S A** 102(16):5844–5849, 2005.
 35. Levin VA, Silver P, Hannigan J, Wara WM, Gutin PH, Davis RL, et al.: Superiority of post-radiotherapy adjuvant chemotherapy with CCNU, procarbazine, and vincristine (PCV) over BCNU for anaplastic gliomas: NCOG 6G61 final report. **Int J Radiat Oncol Biol Phys** 18(2):321–324, 1990.
 36. Sinha R, Kiley SC, Lu JX, Thompson HJ, Moraes R, Jaken S, et al.: Effects of methylselenocysteine on PKC activity, cdk2 phosphorylation and gadd gene expression in synchronized mouse mammary epithelial tumor cells. **Cancer Lett** 146(2):135–145, 1999.
 37. Goan YG, Zhou B, Hu E, Mi S, Yen Y: Overexpression of ribonucleotide reductase as a mechanism of resistance to 2,2-difluorodeoxycytidine in the human KB cancer cell line. **Cancer Res** 59(17):4204–4207, 1999.
 38. Stracker TH, Carson CT, Weitzman MD: Adenovirus oncoproteins inactivate the Mre11-Rad50-NBS1 DNA repair complex. **Nature** 418(6895):348–352, 2002.
 39. Srivenugopal KS, Shou J, Mullapudi SR, Lang FF, Jr., Rao JS, Ali-Osman F: Enforced expression of wild-type p53 curtails the transcription of the O(6)-methylguanine-DNA methyltransferase gene in human tumor cells and enhances their sensitivity to alkylating agents. **Clin Cancer Res** 7(5):1398–1409, 2001.
 40. Batchelor TT, Betensky RA, Esposito JM, Pham LD, Dorfman MV, Piscatelli N, et al.: Age-dependent prognostic effects of genetic alterations in glioblastoma. **Clin Cancer Res** 10(1 Pt 1):228–233, 2004.
 41. Kanzawa T, Bedwell J, Kondo Y, Kondo S, Germano IM: Inhibition of DNA repair for sensitizing resistant glioma cells to temozolomide. **J Neurosurg** 99(6):1047–1052, 2003.
 42. Kramm CM, Chase M, Herrlinger U, Jacobs A, Pechan PA, Rainov NG, et al.: Therapeutic efficiency and safety of a second-generation replication-conditional HSV1 vector for brain tumor gene therapy. **Hum Gene Ther** 8(17):2057–2068, 1997.